МАТЕМАТИЧНІ МЕТОДИ, МОДЕЛІ,
ПРОБЛЕМИ І ТЕХНОЛОГІЇ ДОСЛІДЖЕННЯ
СКЛАДНИХ СИСТЕМ

UDC 519.004.942
DOI: 10.20535/SRIT.2308-8893.2020.3.09

SIMULATING THE ROTATION OF A BLACK HOLE AND ANTIGRAVITY

Y. MATSUKI, P.I. BIDYUK

Abstract. In this article we show that rotation of a black hole can create antigravity and anti-gravitational waves, given that there is a strong gravity in the black hole, which distorts time and space. At first, we derived the curvature tensors upon Einstein's field equation, using spherical polar coordinates, and then calculated the coefficients of the curvature tensors to simulate the strength of each component of the tensors. It is assumed that the stress-energy tensor, which is located outside of the black hole, can reflect the strength of the gravitational field and the gravitational waves. As the result, we concluded that, if the time and space are distorted in the black hole, the rotation can create antigravity and the anti-gravitational waves. In addition, the result of the simulation shows that the antigravity positively contributes to the stress-energy tensor, which may expand the size of the Universe.

Keywords: antigravity, curvature tensor, stress-energy tensor, Einstein's field equation.

INTRODUCTION (RESEARCH QUESTION)

In our previous two researches [1, 2], we reported as follows: the negative flow of gravitational waves (anti-gravitational waves) must be described by the expression: $-g^{\mu\nu}g_{\rho\sigma,\mu\nu}=0$, while Dirac [3] predicted that, $g^{\mu\nu}g_{\rho\sigma,\mu\nu}=0$, describes the gravitational waves. This means that the negative waves move backward from the direction of the positive flow of the waves. Usually the positive flow and the negative flow should be balanced; therefore, neither of the positive flow nor negative flow of gravitational waves is observable. However, when a star moves, the movement of the mass of the star breaks the balance; and then gravitational waves of both positive and negative flows appear [1]. Upon this conclusion, we investigated the curvature tensors of gravitational waves that are emitted from a black hole and found that the tensors of the gravitational waves from a black hole share the same mathematical forms with the tensors of gravitational field of the black hole [2].

And then, we made the next research to investigate the effect of rotation of the black hole, assuming that the rotation of the black hole breaks the balance of positive and negative flows so that anti-gravitational waves would appear. We also examined, whether or not, the antigravity appears when the black hole rotates and this antigravity creates the energy that may expand size of the Universe to larger scale. This article reports the results of these investigations.

CURVATURE TENSORS FOR SIMULATION

Gravitational field

According to Einstein and Dirac [3], the gravitational field is described by the curvature tensors:

$$R_{\mu\nu} = \Gamma^{\alpha}_{\mu\alpha,\nu} - \Gamma^{\alpha}_{\mu\nu,\alpha} - \Gamma^{\alpha}_{\mu\nu}\Gamma^{\beta}_{\alpha\beta} + \Gamma^{\alpha}_{\mu\beta}\Gamma^{\beta}_{\nu\alpha},$$

where

$$\Gamma^{\lambda}_{\mu\nu} = g^{\lambda\alpha}\Gamma_{\alpha\mu\nu} = \frac{1}{2} g^{\lambda\alpha}(g_{\alpha\mu,\nu} + g_{\alpha\nu,\mu} - g_{\mu\nu,\alpha}). \quad (1)$$

Here, $g^{\lambda\alpha}$, are the fundamental tensors that describe the curvature of the 4-dimensional space in spherical polar coordinates, which is diagonal and symmetric as shown below:

$$g^{\lambda\alpha} = \begin{bmatrix} g^{00} & g^{01} & g^{02} & g^{03} \\ g^{10} & g^{11} & g^{12} & g^{13} \\ g^{20} & g^{21} & g^{22} & g^{23} \\ g^{30} & g^{31} & g^{32} & g^{33} \end{bmatrix} =$$

$$= \begin{bmatrix} 1 & 0 & 0 & 0 \\ 0 & -\dfrac{2m}{\mu(\rho-\tau)^{\frac{2}{3}}} & 0 & 0 \\ 0 & 0 & -\mu^2(\rho-\tau)^{\frac{4}{3}} & 0 \\ 0 & 0 & 0 & -\mu^2(\rho-\tau)^{\frac{4}{3}}\sin^2\theta \end{bmatrix}.$$

And it makes the geodesic of the kind:

$$\Gamma^{\alpha}_{\mu\nu} = g^{\alpha\alpha}\Gamma_{\alpha\mu\nu} = \frac{1}{2} g^{\alpha\alpha}(g_{\alpha\mu,\nu} + g_{\alpha\nu,\mu} - g_{\mu\nu,\alpha}).$$

Therefore, the equation (1) becomes like this: $\Gamma^{\alpha}_{\mu\nu} = g^{\alpha\alpha}\Gamma_{\alpha\mu\nu} =$ $= \frac{1}{2} g^{\alpha\alpha}(g_{\alpha\mu,\nu} + g_{\alpha\nu,\mu} - g_{\mu\nu,\alpha})$, where $g_{\alpha\mu,\nu} = \frac{\partial g_{\alpha\mu}}{\partial x_{\nu}}$, and x_{ν}, is the vector in ν-th coordinate.

Then, we derived all the components of, $R_{\mu\nu}$, and then according to Einstein's rule ($R_{\mu\nu} = \sum_{\mu\nu} R_{\mu\nu}$), summated them to obtain:

$$R_{00} = \frac{-11}{9(\rho-\tau)^2};\ R_{01} = R_{10} = \frac{-4}{9(\rho-\tau)^2},\ R_{11} = \frac{20}{3(\rho-\tau)^2} + \frac{11\mu}{18m(\rho-\tau)^{4/3}};$$

$$R_{22} = \frac{28}{9\mu^2(\rho-\tau)^{10/3}} + \frac{140m}{9\mu^2(\rho-\tau)^4} + \frac{4}{\sin^2\theta} + \cot^2\theta;$$

$$R_{33} = \frac{-28}{9\mu^2(\rho-\tau)^{\frac{10}{3}}\sin^2\theta} + \frac{140m}{9\mu^3(\rho-\tau)^4\sin^2\theta} + \frac{4}{\sin^2\theta} + \frac{11\cot^2\theta}{\sin^2\theta}.$$

Here, μ and m are constants, where, $\mu = (3/2\sqrt{2m})^{2/3}$. All other, $R_{\mu\nu} = 0$. The non-diagonal components, R_{01} and R_{10}, appear because τ and ρ are not independent. However, in this research only the space components of the curvature tensors, R_{11}, R_{22}, and R_{33}, are considered.

Gravitational waves

The curvature tensors of gravitational waves, which penetrate the boundary of a black hole [2], are:

$$g^{\varsigma\eta}{}_{\rho\sigma,\varsigma\eta} + g^{\varsigma\eta}_{,\sigma}(g_{\rho\varsigma,\eta} - \frac{1}{2}g_{\varsigma\eta,\rho}) + g^{\varsigma\eta}_{,\rho}(g_{\sigma\varsigma,\eta} - \frac{1}{2}g_{\varsigma\eta,\sigma}) +$$

$$+\frac{1}{2}g^{\rho\varsigma}g_{\beta\beta}g_{\rho\varsigma,\beta}g_{\eta\varsigma,\beta\sigma} + \frac{1}{2}g^{\rho\varsigma}g_{\beta\beta}g_{\rho\varsigma,\beta\sigma}g_{\eta\varsigma,\beta} +$$

$$+\frac{1}{2}g^{\rho\varsigma}_{,\sigma}g_{\beta\beta}g_{\rho\varsigma,\beta}g_{\eta\varsigma,\beta} + \frac{1}{2}g^{\rho\varsigma}g_{\beta\beta,\sigma}g_{\rho\varsigma,\beta}g_{\eta\varsigma,\beta} +$$

$$+\frac{1}{2}g^{\sigma\varsigma}g_{\beta\beta}g_{\sigma\varsigma,\beta}g_{\varsigma\eta,\beta\rho} + \frac{1}{2}g^{\sigma\varsigma}g_{\beta\beta}g_{\sigma\varsigma,\beta\rho}g_{\varsigma\eta,\beta} +$$

$$+\frac{1}{2}g^{\sigma\varsigma}_{,\rho}g_{\beta\beta}g_{\sigma\varsigma,\beta}g_{\eta\varsigma,\beta} + \frac{1}{2}g^{\sigma\varsigma}g_{\beta\beta,\rho}g_{\sigma\varsigma,\beta}g_{\eta\varsigma,\beta}.$$

When $\varsigma = \eta = 0$: $\frac{4\mu}{9m(\rho-\tau)^{4/3}} - \frac{112}{9\mu^2(\rho-\tau)^{10/3}} - \frac{112}{9\mu^2(\rho-\tau)^{10/3}\sin^2\theta}$;

When $\varsigma = \eta = 1$: $\frac{-16}{9(\rho-\tau)^2} - \frac{2}{3(\rho-\tau)^2} - \frac{2\mu}{81m(\rho-\tau)^{10/3}} + \frac{\mu}{9m(\rho-\tau)^{7/3}} -$

$$-\frac{\mu}{9m(\rho-\tau)^{4/3}} - -\frac{2}{(\rho-\tau)^2} + \frac{224m}{9\mu^3(\rho-\tau)^4} + \frac{224m}{9\mu^3(\rho-\tau)^4\sin^2\theta};$$

When $\varsigma = \eta = 2$: $\frac{24\cos\theta}{\sin^4\theta} + \frac{8}{\sin^2\theta}$, when, $\varsigma = \eta = 3$: $\frac{64}{9(\rho-\tau)^2} - 32\cot^2\theta$.

Distortion of time and space in strong gravity

Using the curvature tensors, Dirac [3] invented a coordinate system that describes the gravitational field from the center of strong gravity in a black hole, in which time and space are distorted by affecting each other. He suggested that if we travel toward the center of the strong gravity, it takes infinite time to reach the center. Upon this Dirac's prescription, we assumed that the time and the distance between the center of the gravitational field and the edge of the Universe are as shown in Fig. 1 and Fig. 2.

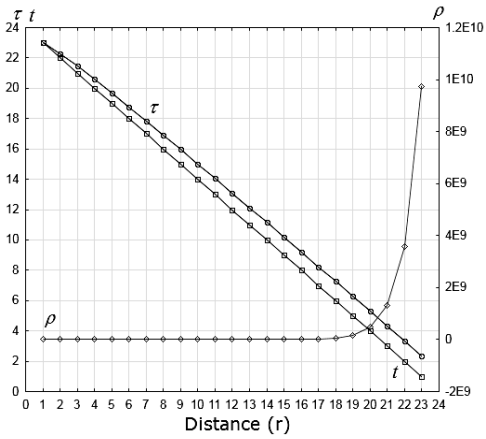

Fig. 1. Time and distance from the center of the gravitational field, Case-1 (non-linear distortion): $f(r) = \log r$ and $g(r) = e^r$

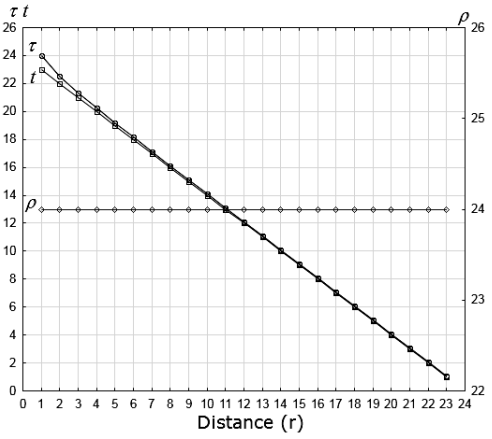

Fig. 2. Time and distance from the center of the gravitational field, Case-2 (linear distortion): $f(r) = (1/4)$ and $g(r) = r$

In these figures, τ is a relative time in the coordinate system, which expands and shrinks depending on the distance r, where $\tau = t + f(r)$; and ρ is the relative distance, which expands and shrinks depending on the time t, where $\rho = t + g(r)$; and $f(r)$, and $g(r)$ are functions of r. For the simulation, we assumed Case 1: $f(r) = \log r$, and, $g(r) = e^r$; and Case 2: $f(r) = \frac{1}{r}$, and $g(r) = r$.

Note: r is the distance from the center of strong gravity, t is the time to travel on the distance, f and g are given functions, and $\tau = t + f(r)$; and $\rho = t + g(r)$.

ALGORITHM

Einstein's field equation [3] that rules the motion of particles in the gravitational field is as follows: $(R^{\mu\nu} - \frac{1}{2} g^{\mu\nu} R)_{,\nu} = 0$. Then, $R_{\mu\nu} - \frac{1}{2} g_{\mu\nu} R = kT$, where T is the stress-energy tensor and k is a constant [4]. Then, we propose the following algorithm to calculate the relative intensities of the components of curvature tensors:

$$H = kT - R_{\mu\nu} = kT - (c_1 X_1 + c_2 X_2 + \cdots + c_l X_l),$$

and

$$H^2 = \{kT - (c_1 X_1 + c_2 X_2 + \cdots + c_1 X_l)\}^2,$$

where $c_1, \ldots, c_l$ are the coefficients, that create a column vector, c. And, $X = [X_1 \quad X_2 \cdots X_l]$, then $H = kT - Xc$. Then we set the constraint, $X'H = 0$, then $X'(kT - Xc) = 0$, where X' is transpose matrix of X.

Then, $X'Xc = X'kT$, $c = (X'X)^{-1} X'kT$, and $\Sigma = V(c) = \sigma^2 (X'X)^{-1}$, where $V(c) = \sigma^2$ is the variance of the c, and $\sigma^2 = e'e/(n-l)$, where $e = MkT$, $M = I - X(X'X)^{-1}X'$; n is the number of rows of each column of X (in this

simulation $n = 23$); l is the number of columns of X; I is a 23×23 unit matrix that holds 1 on all diagonal elements and 0 for the other elements; $(X'X)^{-1}$ is the inverse matrix of $X'X$; and e' is the transpose vector of e. By calculating c and $V(c)$, we estimated the relative strength of each component of, $R_{\mu\nu}$, to the stress-energy tensor in the system of spherical polar coordinates.

Rotation of the object that contains strong gravity

When an object rotates as shown in Fig. 3, its coordinate system will be transformed by the transformation matrix D of the Euler's angles [4]. For the rotation around one axis, the tensors of the object's coordinate system will be multiplied by: $D = \begin{bmatrix} \cos\varphi & \sin\varphi & 0 \\ -\sin\varphi & \cos\varphi & 0 \\ 0 & 0 & 1 \end{bmatrix}$.

And then the curvature tensor will be transformed to the following form:

$$DR_{\mu\nu} = \begin{bmatrix} \cos\varphi & \sin\varphi & 0 \\ -\sin\varphi & \cos\varphi & 0 \\ 0 & 0 & 1 \end{bmatrix} \cdot \begin{bmatrix} R_{11} & 0 & 0 \\ 0 & R_{22} & 0 \\ 0 & 0 & R_{33} \end{bmatrix} =$$

$$= \begin{bmatrix} \cos\varphi R_{11} & \sin\varphi R_{22} & 0 \\ -\sin\varphi R_{11} & \cos\varphi R_{22} & 0 \\ 0 & 0 & R_{33} \end{bmatrix}.$$

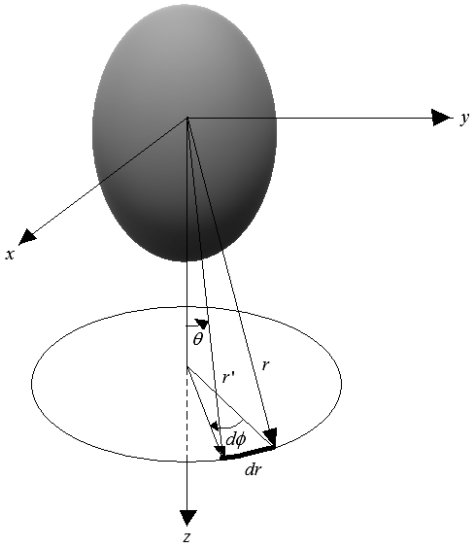

Fig. 3. Rotation of an object

The components of $R_{\mu\nu}$ before and after the rotation are shown in Tables 1 and 2.

For the simulation, we used the components, $\cos\varphi R_{11}$, $\cos\varphi R_{22}$ and R_{33}, which correspond to the coordinates that describe the space coordinates, ρ, θ and φ. The components of R_{33} doesn't change by the rotation, under the operation of $DR_{\mu\nu}$, because $D_{33} = 1$. We selected these three diagonal components for calculating the coefficients of the curvature tensors with the algorithm mentioned above, which simulates the relative strength of each components of the curvature tensor to the stress-energy tensor. However, we didn't use the non-diagonal components, $-\sin\varphi R_{11}$ and $\sin\varphi R_{22}$, because these are perpendicular to the diagonal components, therefore do not contribute to the stress-energy tensor.

SIMULATION

Input data

Time t is set as shown in Fig. 1 for Case-1, and in Fig. 2 for Case-2, with which its slope to the distance, r, from the center of the gravitational field is a constant. For simulating the spatial expansion of the gravitational field, we assumed as if θ becomes larger in far distance. On the other hand, for simulating the flow of gravitational waves, we assumed that θ becomes smaller in far distance, as shown in Fig. 4. For simulating the rotation of the object, we set two cases, assuming φ_1 (Rotation1) and φ_2 (Rotation 2) also as shown in Fig.4. With these settings, $\sin\theta$, $\cos\theta$, $\cot\theta$, and $\cos\varphi$ of the gravitational field behave like as shown in Fig. 5.

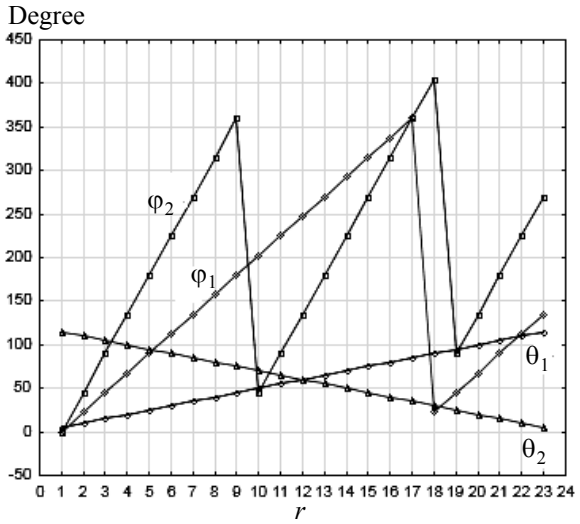

Fig. 4. Angles θ and φ for simulating gravitational field and gravitational waves

Note: θ_1: for gravitational field, θ_2: for gravitational waves, φ_1: for the rotation 1, φ_2: for the rotation 2

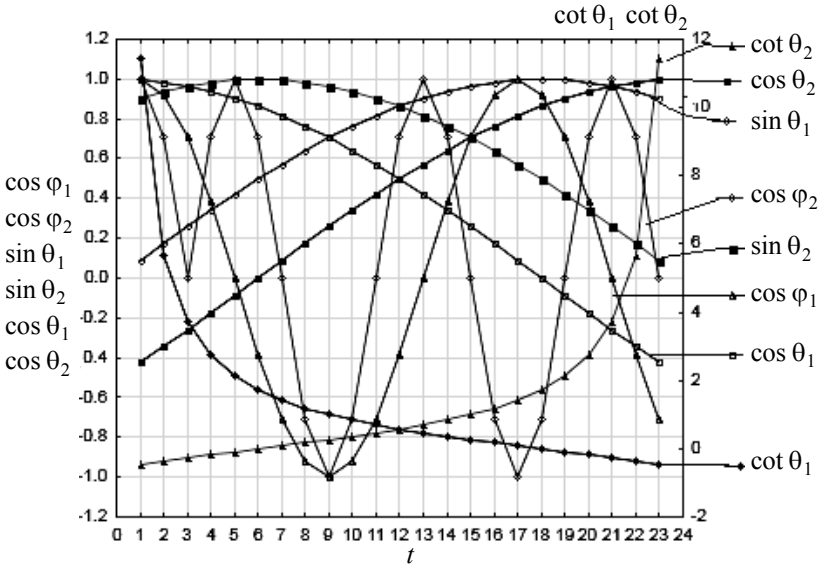

Fig. 5. $\mathrm{Sin}\theta$, $\cos\theta$, $\cot\theta$, and $\cos\varphi$ of the simulated gravitational field

In addition, for this simulation, we set the stress-energy tensor kT to be 1; because, the purpose of this simulation is to measure the order of magnitude of the relative strength of each component of, $R_{\mu\nu}$, to the stress-energy tensor.

RESULTS

Gravitational field

The results of simulation for the gravitational filed are shown in Table 1 for Case-1, and Table 2 for Case-2. The both Tables show the calculated coefficients of the simulation with no rotation, with the rotation 1 and the rotation 2.

T a b l e 1. Results of the simulation of gravitational field, Case-1

Components of $R_{\mu\nu}$	**c and $\sqrt{V(c)}$ of $R_{\mu\nu}$ before the rotation**	**Components of $DR_{\mu\nu}$**	**c and $\sqrt{V(c)}$ (Rotation 1)**	**c and $\sqrt{V(c)}$ (Rotation 2)**
$\frac{1}{(\rho-\tau)^2}$	$2{,}902\cdot10^{-2}$ $(1{,}875\cdot10^{4})$	$\frac{\cos\varphi}{(\rho-\tau)^2}$	$-4{,}255\cdot10^{5}$ $(5{,}078\ \mathrm{i}\cdot10^{5})$	$1{,}783\cdot10^{5}$ $(7{,}302\cdot10^{5})$
$\frac{1}{(\rho-\tau)^{4/3}}$	$3{,}496\cdot10^{-3}$ $(2{,}573\cdot10^{3})$	$\frac{\cos\varphi}{(\rho-\tau)^{4/3}}$	$1{,}390\cdot10^{4}$ $(9{,}997\cdot10^{3})$	$-6{,}495\cdot10^{3}$ $(2{,}272\cdot10^{4})$
$\frac{1}{(\rho-\tau)^{10/3}}$	$-1{,}488\cdot10^{2}$ $(1{,}064\cdot10^{7})$	$\frac{\cos\varphi}{(\rho-\tau)^{10/3}}$	$-2{,}768\cdot10^{7}$ $(1{,}608\mathrm{i}\cdot10^{8})$	$-2{,}996\cdot10^{7}$ $(1{,}004\cdot10^{8})$
$\frac{1}{(\rho-\tau)^{4}}$	$-2{,}623\cdot10^{3}$ $(1{,}808\ \mathrm{i}\cdot10^{8})$	$\frac{\cos\varphi}{(\rho-\tau)^{4}}$	$-2{,}676\cdot10^{8}$ $(8{,}577\ \mathrm{i}\cdot10^{8})$	$1{,}351\cdot10^{8}$ $(4{,}202\cdot10^{8})$
$\frac{1}{\sin^2\theta}$	$1{,}000$ $(6{,}252\cdot10^{-2})$	$\frac{\cos\varphi}{\sin^2\theta}$	$0{,}7787$ $(0{,}3866)$	$0{,}2913$ $(0{,}4413)$
$\cot^2\theta$	$-1{,}000$ $(0{,}5245)$	$\cos\varphi\cdot\cot^2\theta$	$-2{,}788$ $(0{,}7892)$	$-0{,}7126$ $(1{,}432)$
$\frac{1}{(\rho-\tau)^4\sin^2\theta}$	$-55{,}86$ $(3{,}877\ \mathrm{i}\cdot10^{6})$	$\frac{1}{(\rho-\tau)^4\sin^2\theta}$ *	$-6{,}454\cdot10^{6}$ $(2{,}594\ \mathrm{i}\cdot10^{7})$	$-6{,}129\cdot10^{5}$ $(2{,}190\cdot10^{6})$
$-\frac{1}{(\rho-\tau)^{10/3}\sin^2\theta}$	$-38{,}63$ $(2{,}688\ \mathrm{i}\cdot10^{6})$	$-\frac{1}{(\rho-\tau)^{10/3}\sin^2\theta}$ *	$-4{,}436\cdot10^{6}$ $(1{,}736\ \mathrm{i}\cdot10^{7})$	$-1{,}686\cdot10^{4}$ $(2{,}473\cdot10^{5})$
$\frac{\cot^2\theta}{\sin^2\theta}$	$-2{,}773\cdot10^{-7}$ $(0{,}2009)$	$\frac{\cot^2\theta}{\sin^2\theta}$ *	$2{,}057\cdot10^{-2}$ $(0{,}2481\ \mathrm{i})$	$0{,}2367$ $(0{,}1400)$

The values in the brackets are $\sqrt{V(c)}$. For example, $1{,}808\ \mathrm{i}\cdot10^{8} = \sqrt{-3.27\cdot10^{16}}$.

* This component corresponds to the coordinate of the axis of the rotation, therefore $\cos\varphi$ is not multiplied.

In Case-1 (non-linear distortion of the time and space), the coefficient, c, of $\frac{\cot^2\theta}{\sin^2\theta}$ changes its sign from minus to plus after the rotation of φ_1 (the Rotation 1) and of φ_2 (the Rotation 2). The gravity must be negative, and it is so to the stress-energy tensor when it doesn't rotate, but it becomes positive to the stress-energy tensor after the rotations. This result means that the antigravity appears after the rotation.

Table 2. Results of the simulation of gravitational field, Case-2

Components of $R_{\mu\nu}$	**c and** $\sqrt{V(c)}$ **of** $R_{\mu\nu}$ **before the rotation**	**Components of** $DR_{\mu\nu}$	**c and** $\sqrt{V(c)}$ **(Rotation 1)**	**c and** $\sqrt{V(c)}$ **(Rotation 2)**
$\frac{1}{(\rho-\tau)^2}$	-8,518·10^{-3} (1,896·10^{-2})	$\frac{\cos\varphi}{(\rho-\tau)^2}$	1,278·10^{4} (4,437·10^{3})	5,473·10^{3} (3,900·10^{3})
$\frac{1}{(\rho-\tau)^{4/3}}$	1,217·10^{-3} (2,820·10^{-3})	$\frac{\cos\varphi}{(\rho-\tau)^{4/3}}$	-2,182·10^{3} (7,573·10^{2})	-9,831·10^{2} (6,530·10^{2})
$\frac{1}{(\rho-\tau)^{10/3}}$	0,1086 (0,2162)	$\frac{\cos\varphi}{(\rho-\tau)^{10/3}}$	-6,724·10^{4} (2,833·10^{4})	-3,707·10^{4} (2,353·10^{4})
$\frac{1}{(\rho-\tau)^4}$	-0,2701 (0,5121)	$\frac{\cos\varphi}{(\rho-\tau)^4}$	9,317·10^{4} (4,145·10^{4})	4,968·10^{4} (3,173·10^{4})
$\frac{1}{\sin^2\theta}$	1,000 (1,864·10^{-5})	$\frac{\cos\varphi}{\sin^2\theta}$	16,76 (5,815)	8,595 (4,914)
$\cot^2\theta$	-1,000 (2,679·10^{-5})	$\cos\varphi\cdot\cot^2\theta$	-33,90 (9,405)	-9,779 (9,921)
$\frac{1}{(\rho-\tau)^4\sin^2\theta}$	-2,229·10^{-4} (4,083·10^{-4})	$\frac{1}{(\rho-\tau)^4\sin^2\theta}$ *	-1,052·10^{-3} (5,370·10^{2})	-6,204·10^{2} (4,183·10^{2})
$-\frac{1}{(\rho-\tau)^{10/3}\sin^2\theta}$	-3,371·10^{-3} (5,829·10^{-3})	$-\frac{1}{(\rho-\tau)^{10/3}\sin^2\theta}$ *	-2,856·10^{2} (1,743·10^{2})	-3,109·10^{2} (2,104·10^{2})
$\frac{\cot^2\theta}{\sin^2\theta}$	-1,707·10^{-8} (6,560·10^{-8})	$\frac{\cot^2\theta}{\sin^2\theta}$ *	0,1293 (3,106·10^{2})	8,552·10^{-3} (4,746·10^{2})

The values in the brackets are $\sqrt{V(c)}$. For example, 1,808 i $\cdot 10^8 = \sqrt{-3.27\cdot 10^{16}}$.

* This component corresponds to the coordinate of the axis of the rotation, therefore $\cos\varphi$ is not multiplied.

In addition, the coefficients of $\frac{1}{(\rho-\tau)^4}$ and $\frac{\cot^2\theta}{\sin^2\theta}$ change these signs from minus to plus, only for the rotation of φ_2 in Case-1. And in Case-2 (linear distor-

tion of time and space), only the coefficients of $\frac{1}{(\rho-\tau)^2}$, $\frac{1}{(\rho-\tau)^4}$, and $\frac{\cot^2\theta}{\sin^2\theta}$, change these signs from minus to plus after the both rotations of, φ_1, and φ_2.

The summation of each of the positive coefficients and the negative coefficients are shown in Table 5, and in Fig. 6 for Case-1, and Fig. 7 for Case-2. In case of non-linear distortion of time and space (Case-1), antigravity appears after the Rotation 2 in Case-1; while in case of linear distortion of time and space (Case-2), the antigravity appears after both of the Rotation 1 and 2.

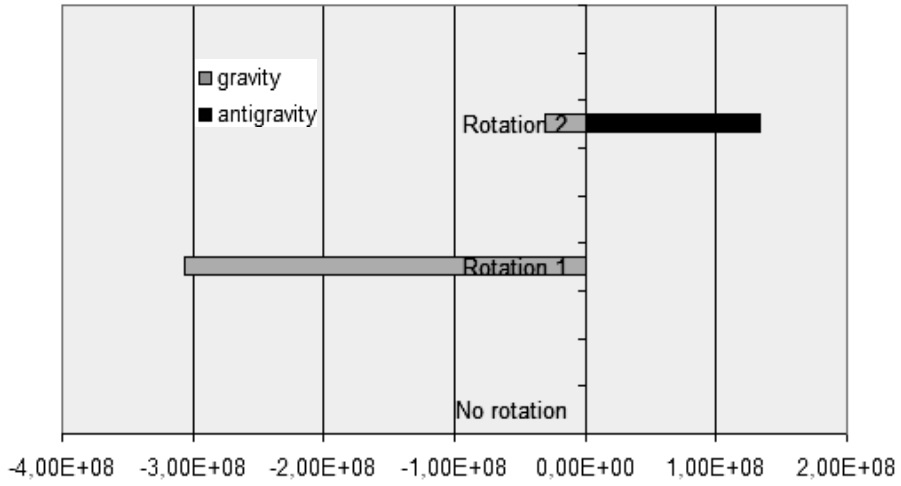

Fig. 6. Gravity and antigravity (Case – 1: non-linear distortion of time and space)

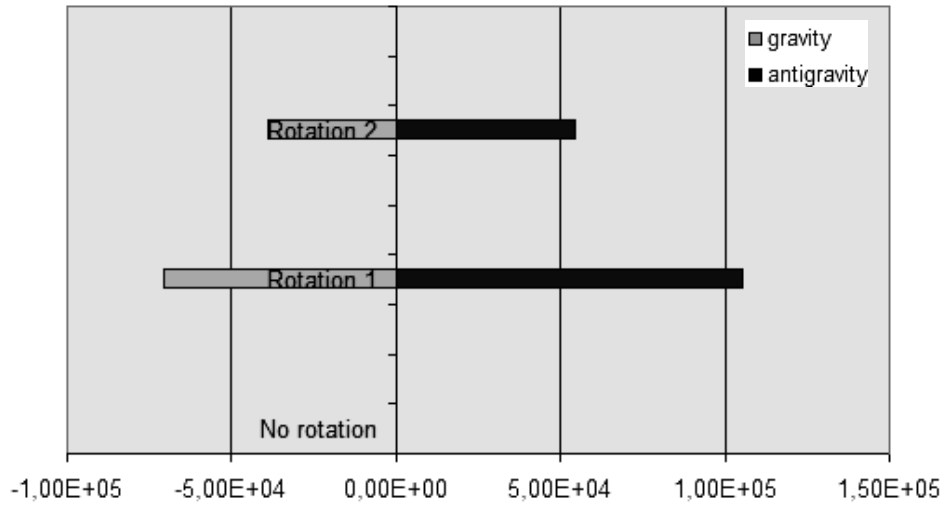

Fig. 7. Gravity and antigravity (Case – 2: linear distortion of time and space)

Gravitational waves

The results of simulation for the gravitational waves are shown in Table 3 for Case-1 and Table 4 for Case-2. For the gravitational waves the coefficients of the

curvature tensors are positive to the stress-energy tensor; while the negative coefficients represent the anti-gravitational waves.

Table 3. Results of the simulation of gravitational waves, Case-1

Components of gravitational waves before the rotation	**c and $\sqrt{V(c)}$ of gravitational waves**	**Components of gravitational waves after the rotation**	**c and $\sqrt{V(c)}$ Rotation 1**	**c and $\sqrt{V(c)}$ Rotation 2**
$\frac{1}{(\rho-\tau)^2}$	$1{,}200\cdot10^{4}$ $(6{,}038\cdot10^{-8})$	$\frac{\cos\varphi}{(\rho-\tau)^2}$	$1{,}185\cdot10^{6}$ $(3{,}619\cdot10^{10})$	$-1{,}210\cdot10^{6}$ $(3{,}772\ \mathrm{i}\cdot10^{9})$
$\frac{1}{(\rho-\tau)^{4/3}}$	-84,48 $(5{,}520\cdot10^{6})$	$\frac{\cos\varphi}{(\rho-\tau)^{4/3}}$	$-1{,}723\cdot10^{4}$ (7,669)	$9{,}443\cdot10^{3}$ $(8{,}600\ \mathrm{i}\cdot10^{6})$
$\frac{1}{(\rho-\tau)^{4}}$	$1{,}360\cdot10^{7}$ $(9{,}263\ \mathrm{i}\cdot10^{11})$	$\frac{\cos\varphi}{(\rho-\tau)^{4}}$	$1{,}450\cdot10^{9}$ $(6{,}839\ \mathrm{i}\cdot10^{13})$	$9{,}839\cdot10^{-8}$ $(5{,}481\ \mathrm{i}\cdot10^{12})$
$\frac{1}{\sin^2\theta}$	1,001 $(1{,}747\cdot10^{2})$	$\frac{\cos\varphi}{\sin^2\theta}$	0,1496 $(1{,}703\cdot10^{3})$	$2{,}997\cdot10^{-2}$ $(1{,}422\cdot10^{2})$
$-\cot^2\theta$	-1,001 $(1{,}877\cdot10^{-2})$	$-\cot^2\theta$ *	$8{,}722\cdot10^{-2}$ $(6{,}337\cdot10^{-2})$	$8{,}884\cdot10^{-3}$ (11,21)
$\frac{1}{(\rho-\tau)^4\sin^2\theta}$	$-6{,}752\cdot10^{6}$ $(4{,}939\ \mathrm{i}\cdot10^{11})$	$\frac{\cos\varphi}{(\rho-\tau)^4\sin^2\theta}$	$-7{,}830\cdot10^{-8}$ $(4{,}291\ \mathrm{i}\cdot10^{13})$	$-8{,}148\cdot10^{-8}$ $(4{,}387\ \mathrm{i}\cdot10^{12})$
$-\frac{1}{(\rho-\tau)^{10/3}\sin^2\theta}$	$1{,}476\cdot10^{7}$ $(7{,}651\ \mathrm{i}\cdot10^{11})$	$-\frac{\cos\varphi}{(\rho-\tau)^{10/3}\sin^2\theta}$	$1{,}293\cdot10^{9}$ $(2{,}133\ \mathrm{i}\cdot10^{13})$	$-3{,}424\cdot10^{-8}$ $(2{,}597\ \mathrm{i}\cdot10^{12})$
$-\frac{1}{(\rho-\tau)^{10/3}}$	$-1{,}544\cdot10^{7}$ $(7{,}783\ \mathrm{i}\cdot10^{11})$	$-\frac{\cos\varphi}{(\rho-\tau)^{10/3}}$	$-1{,}335\cdot10^{9}$ $(1{,}668\ \mathrm{i}\cdot10^{13})$	$4{,}209\cdot10^{-8}$ $(2{,}913\ \mathrm{i}\cdot10^{12})$
$\frac{1}{(\rho-\tau)^{7/3}}$	$-4{,}509\cdot10^{4}$ $(1{,}953\cdot10^{9})$	$\frac{\cos\varphi}{(\rho-\tau)^{7/3}}$	$-3{,}890\cdot10^{6}$ $(1{,}437\cdot10^{11})$	$4{,}601\cdot10^{6}$ (1,723 i
$\frac{\cos\theta}{\sin^4\theta}$	$2{,}996\cdot10^{7}$ (0,1763)	$\frac{\cos\varphi\cdot\cos\theta}{\sin^4\theta}$	$-2{,}889\cdot10^{-4}$ (11,36)	$1{,}859\cdot10^{4}$ (5,165)
–	–	$\frac{1}{(\rho-\tau)^2}$ *	$1{,}876\cdot10^{4}$ $(6{,}619\cdot10^{3})$	$3{,}842\cdot10^{-2}$ $(5{,}644\cdot10^{5})$

The values in the brackets are $\sqrt{V(c)}$. For example, $1{,}808\ \mathrm{i}\cdot10^{8} = \sqrt{-3.27\cdot10^{16}}$.

* This component corresponds to the coordinate of the axis of the rotation, therefore $\cos\varphi$ is not multiplied.

Table 4. Results of the simulation of gravitational waves, Case-2

Components of gravitational waves before the rotation	c and $\sqrt{V(c)}$ of gravitational waves	Components of gravitational waves after the rotation	c and $\sqrt{V(c)}$ Rotation 1	c and $\sqrt{V(c)}$ Rotation 2
$\frac{1}{(\rho-\tau)^2}$	$2{,}335\cdot10^{-2}$ (21,38)	$\frac{\cos\varphi}{(\rho-\tau)^2}$	$-2{,}080\cdot10^{4}$ ($7{,}251\cdot10^{3}$)	$3{,}964\cdot10^{3}$ ($1{,}428\cdot10^{4}$)
$\frac{1}{(\rho-\tau)^{4/3}}$	$-1{,}708\cdot10^{-3}$ (1,511)	$\frac{\cos\varphi}{(\rho-\tau)^{4/3}}$	$1{,}220\cdot10^{3}$ ($4{,}052\cdot10^{-3}$)	$-5{,}052\cdot10^{2}$ ($9{,}136\cdot10^{2}$)
$\frac{1}{(\rho-\tau)^4}$	1,217 ($1{,}140\cdot10^{3}$)	$\frac{\cos\varphi}{(\rho-\tau)^4}$	$-1{,}463\cdot10^{6}$ ($6{,}858\cdot10^{5}$)	$3{,}541\cdot10^{6}$ ($2{,}825\cdot10^{6}$)
$\frac{1}{\sin^2\theta}$	1,000 ($9{,}834\cdot10^{-4}$)	$\frac{\cos\varphi}{\sin^2\theta}$	0,8678 (0,3550)	0,8594 (0,7481)
$\cot^2\theta$	-1,000 ($2{,}405\cdot10^{-3}$)	$-\cot^2\theta$ *	$5{,}531\cdot10^{-3}$ ($2{,}318\cdot10^{-3}$)	$8{,}384\cdot10^{-3}$ ($6{,}984\cdot10^{-3}$)
$\frac{1}{(\rho-\tau)^4\sin^2\theta}$	-0,9864 ($9{,}137\cdot10^{-2}$)	$\frac{\cos\varphi}{(\rho-\tau)^4\sin^2\theta}$	$1{,}169\cdot10^{6}$ ($5{,}448\cdot10^{5}$)	$-2{,}773\cdot10^{6}$ ($2{,}218\cdot10^{6}$)
$-\frac{1}{(\rho-\tau)^{10/3}\sin^2\theta}$	-0,1682 ($1{,}523\cdot10^{2}$)	$-\frac{\cos\varphi}{(\rho-\tau)^{10/3}\sin^2\theta}$	$1{,}568\cdot10^{5}$ ($6{,}602\cdot10^{4}$)	$-3{,}016\cdot10^{5}$ ($2{,}612\cdot10^{5}$)
$-\frac{1}{(\rho-\tau)^{10/3}}$	0,2770 ($2{,}517\cdot10^{2}$)	$-\frac{\cos\varphi}{(\rho-\tau)^{10/3}}$	$-2{,}829\cdot10^{5}$ ($1{,}292\cdot10^{5}$)	$6{,}841\cdot10^{5}$ ($5{,}614\cdot10^{5}$)
$\frac{1}{(\rho-\tau)^{7/3}}$	$-2{,}439\cdot10^{2}$ (22,20)	$\frac{\cos\varphi}{(\rho-\tau)^{7/3}}$	$2{,}115\cdot10^{4}$ ($8{,}154\cdot10^{3}$)	$2{,}338\cdot10^{4}$ ($2{,}391\cdot10^{4}$)
$\frac{\cos\theta}{\sin^4\theta}$	$8{,}679\cdot10^{-10}$ ($1{,}092\cdot10^{-6}$)	$\frac{\cos\varphi\cdot\cos\theta}{\sin^4\theta}$	$3{,}683\cdot10^{-4}$ ($6{,}707\cdot10^{-4}$)	$-1{,}286\cdot10^{-2}$ ($8{,}520\cdot10^{-3}$)
–	–	$\frac{1}{(\rho-\tau)^2}$ *	30,60 (8,602)	11,74 (6,283)

The values in the brackets are $\sqrt{V(c)}$. For example, 1,808 i $\cdot10^{8} = \sqrt{-3.27\cdot10^{16}}$.

* This component corresponds to the coordinate of the axis of the rotation, therefore $\cos\phi$ is not multiplied.

In Case-1 (non-linear distortion of time and space), the coefficient, c, of, $\frac{\cos\theta}{\sin^4\theta}$, changes its sign from plus to minus after the rotation of φ_1 (the Rotation 1), and, $\frac{1}{(\rho-\tau)^2}$, and $-\frac{1}{(\rho-\tau)^{10/3}\sin^2\theta}$, change these signs from plus to minus after the rotation of φ_2 (the Rotation 2). And in Case-2 (linear distortion of time

and space), the coefficients of $\frac{1}{(\rho-\tau)^2}$, $\frac{1}{(\rho-\tau)^4}$ and $-\frac{1}{(\rho-\tau)^{10/3}}$ change these signs from plus to minus after the rotation of φ_1 (the Rotation 1), while the coefficient of, $\frac{\cos\theta}{\sin^4\theta}$, changes its sing from plus to minus after the rotation of φ_2 (the Rotation 2).

Table 5. Strengths of gravity and antigravity

Case	Case-1		Case-2	
	Gravity	Antigravity	Gravity	Antigravity
No rotation	$-2{,}867\cdot10^3$	1,033	-1,282	1,110
Rotation 1	$-3{,}066\cdot10^8$	$1{,}390\cdot10^4$	$-7{,}079\cdot10^4$	$1{,}060\cdot10^5$
Rotation 2	$-3{,}060\cdot10^7$	$1{,}353\cdot10^8$	$-3{,}899\cdot10^4$	$5{,}516\cdot10^4$

The summation of each of the positive coefficients and the negative coefficients are shown in Table 6, and in Fig. 8 for Case-1, and Fig. 9 for Case-2. In both cases, gravity and antigravity are balanced without the rotation of the black hole, but the balance is broken after the rotations, then antigravity appears with the Rotation 2 in Case-1, and with both of the Rotation 1 and Rotation 2 in Case-2. Also, gravitational waves and anti-gravitational waves are balanced without the rotation, but they appear when the black hole rotates.

Table 6. Strengths of gravitational waves and anti-gravitational waves

Case	Case - 1		Case - 2	
	Gravitational waves	Anti-gravitational waves	Gravitational waves	Anti-gravitational waves
No rotation	$2{,}838\cdot10^7$	$-2{,}224\cdot10^7$	2,517	-2,181
Rotation 1	$2{,}744\cdot10^9$	$-2{,}122\cdot10^9$	$1{,}348\cdot10^6$	$-1{,}766\cdot10^6$
Rotation 2	$1{,}409\cdot10^9$	$-1{,}158\cdot10^9$	$4{,}252\cdot10^6$	$-3{,}075\cdot10^6$

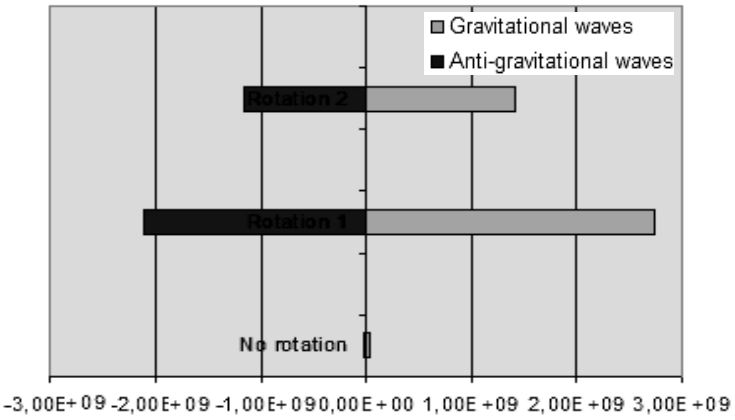

Fig. 8. Gravitational waves and anti-gravitational waves (Case-1: non-linear distortion of time and space)

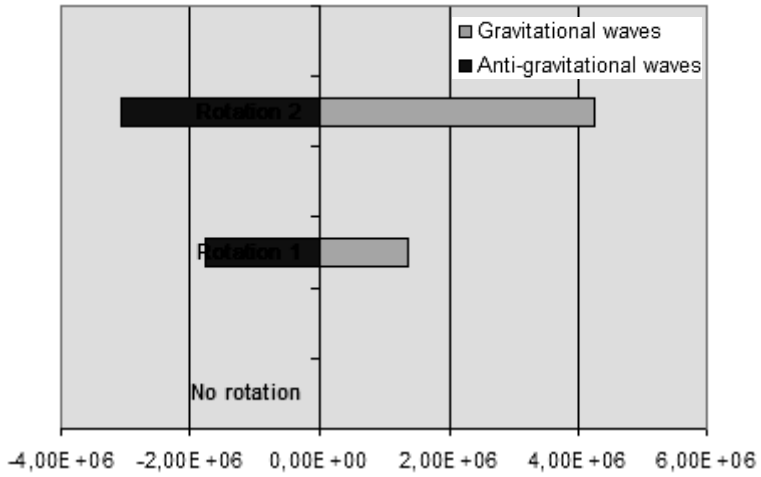

Fig. 9. Gravitational waves and anti-gravitational waves (Case-2: linear distortion of time and space)

PHYSICAL MEANING OF THE RESULT

Here, $R_{\mu\nu} - (1/2)g_{\mu\nu}R + \Lambda g = kT$, is the equation of gravitational field of the Universe [4], where $R_{\mu\nu}$ are curvature tensors, named Ricci tensors, $g_{\mu\nu}$ are fundamental tensors, $R_{\mu\nu} = R$, and, $g_{\mu\nu} = g$, where $\mu = \nu$, T is the stress-energy tensor and k is a constant, and $\Lambda < 0$ is the cosmological constant named "dark energy", which is a positive contribution to kT. The above result of our simulation shows that the rotation of the black hole makes positive contribution to the stress-energy tensor, which may expand the size of the Universe, however it is unknown if the antigravity is related to the dark energy.

Fig. 6 and Fig.7 show that the gravity and the antigravity are balanced without the rotation, but balance is broken when the black hole rotates. Also, Fig. 8 and Fig. 9 show that the gravitational waves and the anti-gravitational waves are balanced without the rotation, but the balance is broken when the black hole rotates. This finding is consistent with our previous report [1].

CONCLUSIONS AND RECOMMENDATIONS

In this simulation, assuming that the coordinates of time and space can be distorted in the strong gravity in a black hole, we investigated whether a rotation of a black hole can produce antigravity and anti-gravitational waves, or not, by calculating the relative strengths of the components of the curvature tensors of the black hole, which are measured by the stress-energy tensor that is placed outside of the black hole, upon Einstein's field equation. In order to simulate the curvature in the strong gravity, we used the system of the spherical polar coordinates so that we could simulate rotation of the black hole with Euler's angles.

The results of the simulation show that the rotating black hole can produce the antigravity and anti-gravitational waves, if time and space are distorted linearly and non-linearly. Also, the results suggest a possible explanation about the expansion of the Universe.

Further investigations are needed about the process of the time-space distortions and of the angular momentum of the rotation.

REFERENCES

1. Y. Matsuki, P.I. Bidyuk, "Analysis of negative flow of gravitational waves (Part 5)", *System Research & Information Technology*, no. 4, pp. 7–18, 2019.
2. Y. Matsuki, P.I. Bidyuk, "Numerical Simulation of Gravitational Waves from a Black hole, using Curvature Tensors (Part 6)", *System Research & Information Technology*, no.1, pp. 54–67, 2020.
3. P.A.M. Dirac, *General Theory of Relativity*, Florida University, A Wiley-Interscience Publication, John Wiley & Sons, New York, 1975, pp. 69 .
4. H. Goldstein, C.P. Poole, J.L. Safko, *Classical Mechanics*, 3rd Edition, published by Pearson Education, Inc., 2002, pp. 646; [especially Chapter 4 "The Kinematics of Rigid Body Motion", pp.134–183, Chapter 7.11 "Introduction to the general theory of relativity", pp. 324–328].

Received 02.07.2020

From the Editorial Board: the article corresponds completely to submitted manuscript.

INFORMATION ON THE ARTICLE

Petro I. Bidyuk, ORCID: 0000-0002-7421-3565, Educational and Scientific Complex "Institute for Applied System Analysis" of the National Technical University of Ukraine "Igor Sikorsky Kyiv Polytechnic Institute", Ukraine, e-mail: pbidyuke_00ukr.net

Yoshio Matsuki, ORCID: 0000-0002-5917-8263, National Technical University of Ukraine "Igor Sikorsky Kyiv Polytechnic Institute", Ukraine, e-mail: matsuki@wdc.org.ua

ІМІТАЦІЙНЕ МОДЕЛЮВАННЯ ОБЕРТАННЯ ЧОРНОЇ ДІРИ ТА АНТИГРАВІТАЦІЇ / Й. Мацукі, П.І. Бідюк

Анотація. Показано, що обертання чорної діри може створити антигравітацію та антигравітаційні хвилі за умови, що у чорній дірі існує сильна гравітація, яка викривлює час і простір. Отримано тензори кривизни на підставі рівняння поля Ейнштейна з використанням сферичних полярних координат, розраховано коефіцієнти тензорів для моделювання сили кожного компонента тензорів. Зроблено припущення, що тензор енергії-імпульсу, розміщений за межами чорної діри, може відображати силу гравітаційного поля і гравітаційних хвиль. У результаті сформовано такий висновок: якщо час і простір викривляються у чорній дірі, то обертання може створити антигравітацію та антигравітаційні хвилі. Результат моделювання показав, що антигравітація робить позитивний внесок у тензор енергії імпульсу, що може розширити розмір Всесвіту.

Ключові слова: антигравітація, тензор кривизни, тензор енергії напруження, рівняння Ейнштейна для поля.

ИМИТАЦИОННОЕ МОДЕЛИРОВАНИЕ ВРАЩЕНИЯ ЧЕРНОЙ ДЫРЫ И АНТИГРАВИТАЦИИ / Й. Мацуки, П.И. Бидюк

Аннотация. Показано, что вращение черной дыры может создать антигравитацию и антигравитационные волны при условии, что в черной дыре существует сильная гравитация, которая искажает время и пространство. Получены тензоры кривизны на основании уравнения поля Эйнштейна с использованием сферических полярных координат, рассчитаны коэффициенты тензоров для моделирования силы каждого компонента тензоров. Предполагается, что тензор энергии импульса, расположенный за пределами черной дыры, может отражать силу гравитационного поля и гравитационных волн. В результате сформулирован вывод: если время и пространство искривляются в черной дыре, вращение может создать антигравитацию и антигравитационные волны. Результат моделирования показал, что антигравитация делает позитивный вклад в тензор энергии импульса, что может расширить размер Вселенной.

Ключевые слова: антигравитация, тензор кривизны, тензор энергии напряжения, уравнение Эйнштейна для поля.